FRESNEL FRINGES DURING THE RECONSTRUCTION OF A HOLOGRAM OF A SCATTERING MEDIUM

A.G. Borovoi, V.V. Demin, N.I. Vagin, and V.A. Donchenko

Institute of Atmospheric Optics,
Siberian Branch of the Russian Academy of Sciences, Tomsk,
V.V. Kuibyshev Tomsk State University,
V.D. Kuznetsov Siberian Physical Technical Institute at the Tomsk State University
Received July 5, 1993

A field reconstructed from a hologram of a scattering medium is theoretically described. The intensity distribution in the focal plane of a lens positioned behind the hologram is analyzed. Two superimposed patterns are shown to be observed in this plane. The first pattern is in complete agreement with a small-angle spectrum of radiation scattered by an ensemble of particles, and its form is independent of distances from the medium to the hologram and lens. The second pattern represents the Fresnel fringes and depends on the distance between the medium and the hologram. The experimental results are presented.

1. INTRODUCTION

Among different methods of optical diagnostics and recording of light scattering media (aerosol, hydrosol, etc.), the holographic method occupies a particular position. Actually, a hologram of a scattering medium enables one to repeatedly reconstruct the optical field scattered by this medium and to extract information about the parameters of macroparticles of the medium. To do this, the particle images reconstructed from the hologram are usually analyzed using an optical system and the most complete information about the size, shape, and location of each particle is obtained. However, such a procedure requires much time and hence is efficient only for ensembles of few particles.

With the hologram of a scattering medium at hand it is possible to combine the procedure of field reconstruction from the hologram with some standard procedure of optical diagnostics of the medium to measure such integral characteristics as particle size distribution in real time. Thus in the experiments described in Refs. 1–3 a small–angle meter of integral particle size distribution was placed immediately behind the illuminated hologram.

It is known however that the field reconstructed from a plane hologram is not fully equivalent to the initial field recorded on the hologram. The reconstructed field consists of two components: initial field and conjugated field. Each of these components may interfere with specific measurements. The interference between these fields may also interfere with such measurements. Moreover, each component can carry supplemental information about the medium, therefore both of these components must be taken into account when interpreting the measurements made in the field reconstructed from the hologram.

The field reconstructed from a plane axial hologram of an ensemble of particles is theoretically considered in sections 2, 3, and 4 of this paper. Both the initial and conjudate fields are shown to produce the same intensity distribution (the Fraunhofer fringes of diffraction by particles) in the focal plane of a lens of the analyzer, e.g., a small–angle meter of particle size distribution. The interference between these fields results in smaller–scale Fresnel fringes which were obviously studied only by us.[4]

The experimental results of observation of the Fresnel fringes are described in section 5.

2. HOLOGRAPHY OF SCATTERING MEDIA

Light fields produced during holography of scattering media are readily described in an analytical form since they represent simply the superposition of spherical waves. On the basis of parabolic equation frequently used in the theory of wave propagation such a spherical wave has the form

$$U_j(x, \rho) = \varphi_j\left(\frac{\rho - \rho_j}{x - x_j}\right) \exp\left[\frac{i\,k\,(\rho - \rho_j)^2}{2(x - x_j)}\right] \Big/ (x - x_j), \quad (1)$$

where $k = 2\pi/\lambda$, λ is the wavelength, x is the longitudinal and $\rho = (y, x)$ is the transverse coordinates, and (x_j, ρ_j) is the point of wave focusing. The multiplier $(x - x_j)^{-1}\exp[ik(\rho - \rho_j)^2/2(x - x_j)]$ describes an isotropic spherical wave, and the angular function φ which varies much more slowly compared to the exponent modulates a spherical wave in amplitude and phase. The angular function φ usually vanishes outside some cone.

It should be noted that formula (1) describes the wave both before the focusing point $x < x_j$ and after it $x > x_j$. Actually, when $x > x_j$, the multiplier $(x - x_j)^{-1}\exp[ik(\rho - \rho_j)^2/2(x - x_j)]$ describes a spherical wave outgoing to the right of the focusing point $x = x_j$.

When the observation point goes over into the region $x < x_j$, the multiplier $x - x_j$ is opposite in sign. Such change of sign of the exponent converts a spherical wave from a divergent to a convergent one. The change of sign of the multiplier $(x - x_j)^{-1}$ is equivalent to wave phase shift by $\pi\,(\exp(i\pi) = -1)$ when passing through the focusing point. This phase shift is well known in optics. As for the change of sign of the multiplier $x - x_j$ entering the argument of the angular function φ, the angular function remains unchanged with simultaneous change of sign of the multiplier $\rho - \rho_j$. This oboiously corresponds to constant value of the angular function on a ray passing through the focusing point.

0235-6880/94/01 27-06 $02.00

From here on, for simplicity, we consider ensembles of particles of radius b which is much larger than the wavelength

$$b \gg \lambda . \tag{2}$$

The generalization to the case $b < \lambda$ should present no problems.

Let a plane wave

$$U_0 = 1 \tag{3}$$

propagating in the direction of the x axis be scattered by a particle centered at the point (x_j, ρ_j). At distances $(x - x_j) > kb^2$, i.e., in the wave zone, the scattered field is described by spherical wave (1) with the angular function being referred to as the scattering amplitude f. It is known that at small scattering angles

$$\Theta = |(\rho - \rho_j) / (x - x_j)| \gtrsim \lambda / b \tag{4}$$

the scattering amplitude is produced by wave diffracted by a particle shadow, i.e., due to diffraction by a black screen formed by particle projection onto the plane x = const

$$f_i(\mathbf{n}) = \frac{i}{\lambda} \int \exp (- i k \mathbf{n} \rho) S_j(\rho) d \rho , \tag{5}$$

$$S_j(\rho) = \begin{cases} 1 \text{ inside the particle shadow,} \\ 0 \text{ outside it,} \end{cases} \tag{6}$$

where $\mathbf{n} = (\rho - \rho_j)/(x - x_j)$. It should be noted that expression (6) is valid for the majority of existing particles. The sole exception is provided by large ($b \gg \lambda$) optically soft particles inside which the run–on of the wave phase does not exceed 2π. This case is said to be anomalous diffraction.

During recording of an axial hologram of scattering media, the superposition of incident (3) and scattered waves arrives at a photographic plate

$$U = 1 + \omega, \tag{7}$$

where the scattered wave is a superposition of waves scattered by individual particles

$$\omega = \sum U_j = \sum \frac{1}{x - x_j} f_j \left(\frac{\rho - \rho_j}{x - x_j} \right) \exp \left[\frac{i k (\rho - \rho_j)^2}{2(x - x_j)} \right]. \tag{8}$$

Photographic blackening is proportional to the field intensity

$$I = |1 + \omega|^2 = 1 + \omega + \omega^* + |\omega|^2 \approx 1 + \omega + \omega^*. \tag{9}$$

The square of the scattered field intensity can be neglected on account of the estimate

$$|U_j| \sim |f_j| / (x - x_j) \leq k b^2 / (x - x_j) \ll 1. \tag{10}$$

When the hologram is reconstructed, i.e. when it is illuminated by plane wave (3), the field behind the hologram, according to Eq. (9), consists of three terms

$$U = 1 + \omega + \tilde{\omega}, \tag{11}$$

where the first term is the incident field, the second term is the field scattered by an ensemble of particles which forms a virtual image, and the third term is additional field produced by the term ω^* on the hologram which forms a real image of the object behind the hologram.

In this case the term ω^* forms the superposition of spherical waves with focal points (κ_j, ρ_j) being symmetric about the points of particle centers (x_j, ρ_j) with respect to the hologram plane. Let us denote the hologram position on the x axis as x_0 both during its recording and reconstructing, then

$$\kappa_j = 2 (x - x_j) + x_j = 2 x - x_j. \tag{12}$$

The field $\tilde{\omega}$ is the superposition of spherical waves

$$\tilde{\omega} = \sum \tilde{U}_j, \tag{13}$$

which are described by expression (1)

$$\tilde{U}_j = \left(- \frac{1}{x - \kappa_j} \right) f_j^* \left(- \frac{\rho - \rho_j}{x - \kappa_j} \right) \exp \left[\frac{i k (\rho - \rho_j)^2}{2 (x - \kappa_j)} \right]. \tag{14}$$

Here the factors (-1), which were absent in Eq. (8), provide for the fulfillment of the condition

$$\tilde{\omega}(x_0, \rho) = \omega^*(x_0, \rho). \tag{15}$$

It should be noted that in the vicinity of the focal point (κ_j, ρ_j) the wave U_j forms a particle image. Therefore, in analogy with the field U_j in the near diffraction zone $|x - \kappa_j| \ll kb^2$, the expression for the scattered field in the form of spherical wave (14) breaks down. This fact is usually unimportant, since the near diffraction zone is small. Moreover, many theoretical results obtained with the use of spherical waves will remain unchanged if we use exact expression for the scattered field.

3. THE RECONSTRUCTED FIELD IN THE FOCAL PLANE OF A LENS

In the known optical method of measuring the particle size distribution, the field scattered by an ensemble of particles is converted with a lens system and then intensity distribution is studied in the focal plane of a lens.

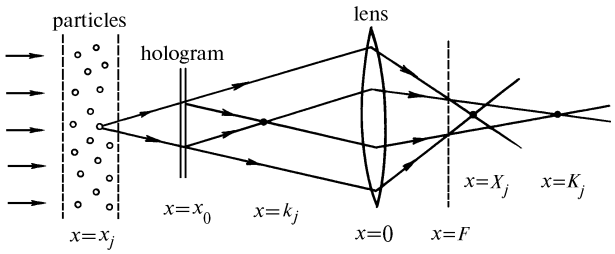

FIG. 1. Optical scheme to the calculation of the intensity distribution in the focal plane of a lens

In this connection let us consider the field described by Eq. (11) and reconstructed from the hologram when it passes through a thin lens. For simplicity we restrict ourselves to the focal plane behind the lens which is of particular interest for practical applications. The center of the lens is taken as the origin of coordinates and the hologram position is denoted by x_0 as before (see Fig. 1).

According to the standard formulas of wave optics, the field U_j in the focal plane is determined by the integral

$$U_j(F, \rho) = \int U_j(0, \rho') \exp\left(-\frac{i\,k\,\rho'^2}{2F}\right)\left(-\frac{i\,k}{2\pi F}\right) \times$$

$$\times \exp\left[\frac{i\,k\,(\rho'-\rho)^2}{2\,F}\right] d\,\rho' , \qquad (16)$$

where F is the focal length, the first exponent describes the phase shift due to the lens, and the remaining multipliers represent the standard Green's function of the wave parabolic equation. After substitution of exact expression for the scattered field, we obtain the integral

$$U_j(F, \rho) = \frac{i\,k}{2\pi\,F\,x_j} \int f_j\left(\frac{\rho_j - \rho'}{x_j}\right) \exp\left[-\frac{i\,k\,(\rho'-\rho_j)^2}{2\,x_j}\right] \times$$

$$\times \exp\left(-\frac{i\,k\,\rho'^2}{2F}\right) \exp\left[\frac{i\,k\,(\rho'-\rho)^2}{2\,F}\right] d\,\rho' . \qquad (17)$$

Let us use some additional considerations to calculate integral (17). On the one hand, it should be noted that integral (17) will be calculated accurately, if we take outside the integral the scattering amplitude, which varies slowly in comparison with exponents, and use the known formula for a two–dimensional Fourier transform of the Gaussian curve

$$\int \exp(\,i\,\alpha\,\rho^2 - i\,\beta\,\rho)\,d\,\rho = \frac{i\,\pi}{\alpha} \exp\left(-\frac{i\,\beta^2}{4\alpha}\right). \qquad (18)$$

As a result, we obtain

$$\frac{i\,k}{2\pi\,F\,x_j} \int \exp\left[-\frac{i\,k\,(\rho'-\rho_j)^2}{2\,x_j}\right] \exp\left(-\frac{i\,k\,\rho'^2}{2\,F}\right) \times$$

$$\times \exp\left[\frac{i\,k\,(\rho'-\rho_j)^2}{2\,F}\right] d\,\rho' = \frac{1}{F} \exp\left[\frac{i\,k\,\rho^2}{2\,(F-X_j)}\right] \exp\left(-\frac{i\,k\,\rho\,\rho_j}{F}\right), \qquad (19)$$

where X_j specifies the position of the image of the point x_j on the x axis determined by the lens formula

$$-\frac{1}{x_j} + \frac{1}{X_j} = \frac{1}{F} . \qquad (20)$$

As could be expected, behind the lens we obtained a spherical wave converging towards the point X_j. The second exponent in Eq. (19) takes into account the displacement of the particle center from the optical axis by way of introducing the exponential multiplier which is typical of the Fourier optics.

On the other hand, the formation of a spherical wave behind the lens is the result of construction of the image by the trivial ray tracing technique within the framework of geometric optics. The angular function, i.e., the scattering amplitude can easy be included into geometrical–optical constructions. It is obvious that the value of the angular function remains constant along rays after they have been refracted by passing through the lens. Therefore, expression (17) for the field behind the lens, taking into account the scattering amplitude, can be written in the same form as Eq. (19) but it must be completed by the scattering amplitude of geometrical–optical rays intersecting the given observation point.

Finally, in the focal plane the field scattered by individual particles takes the form

$$U_j(F, \rho) = \frac{1}{F} f_j\left(\frac{\mathbf{r}}{F}\right) \exp\left[\frac{i\,k\,\mathbf{r}^2}{2(F-X_j)}\right] \exp\left(-\frac{i\,k\,\mathbf{r}\,\mathbf{r}_j}{F}\right). \qquad (21)$$

Now it is easy to write conjugate field (13) in the focal plane of the lens. Actually, the lens transforms spherical wave (1) into a spherical wave whose center of focusing is determined by lens formula (20). It is valid for both divergent $\kappa_j < 0$ or convergent $\kappa_j > 0$ spherical wave incident on the lens. Similar to Eq. (19), when reconstructing the value of the angular function on geometrical–optical rays, we obtain

$$\tilde{U}_j(F, \rho) = \left(-\frac{1}{F}\right) f_j^*\left(-\frac{\rho}{F}\right) \exp\left[\frac{i\,k\,\rho^2}{2(F-K_j)}\right] \exp\left(-\frac{i\,k\,\rho\,\rho_j}{F}\right), \qquad (22)$$

where K_j is the focal point of the wave $\tilde{U}_j$ behind the lens which is found from the formula

$$-\frac{1}{k_j} + \frac{1}{K_j} = \frac{1}{F}.$$

It should be noted that when formula (6) is valid,

$$f^*(-\Theta) = f(\Theta). \qquad (23)$$

4. INTENSITY DISTRIBUTION IN THE FOCAL PLANE OF A LENS

The intensity of the field reconstructed from the hologram is determined by the sum of the terms

$$I = |U_0 + \sum (U_j + \tilde{U}_j)|^2 =$$

$$= |U_0|^2 + 2\mathrm{Re}\,[U_0^* \sum (U_j + \tilde{U}_j)] + \sum |U_j|^2 +$$

$$+ \sum |\tilde{U}_j|^2 + 2\mathrm{Re} \sum U_j\,\tilde{U}_j^* + 2\mathrm{Re} \sum_{j \neq l} (U_j + \tilde{U}_j)(U_l^* + \tilde{U}_l^*) \qquad (24)$$

Consider the intensity distribution in the focal plane of the lens. The incident field converges to a point on the optical axis after passing through a lens; therefore, the first two terms are of no interest to us. The third term, in accordance with Eq. (21), is equal to

$$I_1(F, \rho) = \frac{N}{F^2} \left\langle \left| f\left(\frac{\rho}{F}\right) \right|^2 \right\rangle, \qquad (25)$$

where N is the number of particles, and the statistical averaging <...> is made over all types of particles.

As is seen, the intensity distribution in the focal plane of the lens given by Eq. (25) is independent of the spatial distribution of particles and depends only on their "internal" parameters (size, shape, etc.). Actually, the Fraunhofer diffraction on each particle is observed in the focal plane. If all particles are spherical and of the same size, then the function $I_1(F, \rho)$ describes classical fringes of the Fraunhofer diffraction by a circular disk. For brevity, in the general case distribution (25) is also referred to as the Fraunhofer fringes.

It should be noted that formula (25) is basic in the small–angle method of determining the particle size.

Really, if the *a priori* information about the medium is available, the particle size distribution can be found from the experimental intensity distribution $I_1(F, \rho)$. For example, for spherical particles the form of the function $|f_R(\rho/F)|^2$, where R is the particle radius, is well known. Then formula (25) can be interpreted as an integral transform of the particle size distribution $p(R)$ with the kernel $|f_R(\rho/F)|^2$. The inverse integral transform of the experimental function $I_1(F, \rho)$ yields the unknown function $p(R)$.

Let us now consider the next terms in Eq. (24). As is seen from Eqs. (22) and (23), the fourth term in Eq. (24) fully coincides with the distribution $I_1(F, \rho)$, i.e., the conjugate waves U_j produce exactly the same diffraction pattern in the focal plane. This fact also follows from the ray tracing technique of geometric optics.

Consider now the fifth most interesting term in Eq. (24) which describes the interference between the scattered U_j and conjugate $\tilde{U}_j$ waves. We directly obtain

$$I_{j2} = 2\mathrm{Re}\,(U_j\,\tilde{U}_j^*) =$$

$$= \left(-\frac{2}{F^2}\right)\left|f_j\left(\frac{\rho}{F}\right)\right|^2 \cos\left[\frac{k\,\rho^2}{2}\left(\frac{1}{F-X_j}-\frac{1}{F-K_j}\right)\right]=$$

$$= -\frac{2}{F^2}\left|f_j\left(\frac{\rho}{F}\right)\right|^2 \cos\left[\frac{k\,\rho^2\,(x_0-x_j)}{F^2}\right]. \qquad (26)$$

Thus the interference between the waves U_j and $\tilde{U}_j$ produces an interference pattern in the form of the Fraunhofer fringes modulated by smaller–scale Fresnel fringes.

As far as we know, the appearance of the Fresnel fringes during the reconstruction of holograms of an ensemble of particles was not described in the literature, with the exception of our publication.[4] Let us discuss this fact in greater detail.

As is seen from Eq. (26), the radii of the Fresnel fringes are independent of the distance between the lens and the reconstructed hologram but depend on the distance between a particle and photographic plate during the hologram recording. The radius of the first Fresnel fringe is

$$\rho_1 = \frac{F}{x_0 - x_j}\sqrt{\frac{\lambda\,(x_0-x_j)}{2}}\,, \qquad (27)$$

i.e., this is the radius of the first Fresnel zone on the hologram with the scale factor $F/(x_0 - x_j)$.

When the scattering medium is sufficiently extended along the x axis, the Fresnel fringes are no longer observed due to averaging. Therefore, the most sharp Fresnel fringes can be observed when the scattering medium is either a sufficiently thin layer or a monolayer of particles.

To complete the description of the pattern in the focal plane, we must consider the last term in Eq. (24) which describes the interference between the fields scattered by different particles. It is clear that due to the chaotic phase difference between these waves, the interference pattern corresponding to the last term has a form of irregular spots (specles) which do not alter, on the average, the regular diffraction pattern $(I_1 + I_2)$ in the focal plane.

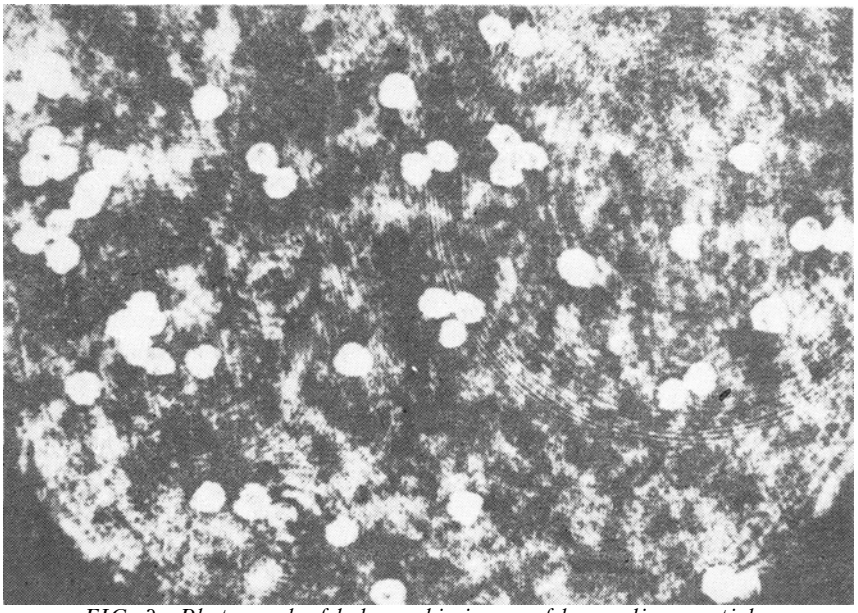

FIG. 2. Photograph of holographic image of lycopodium particles

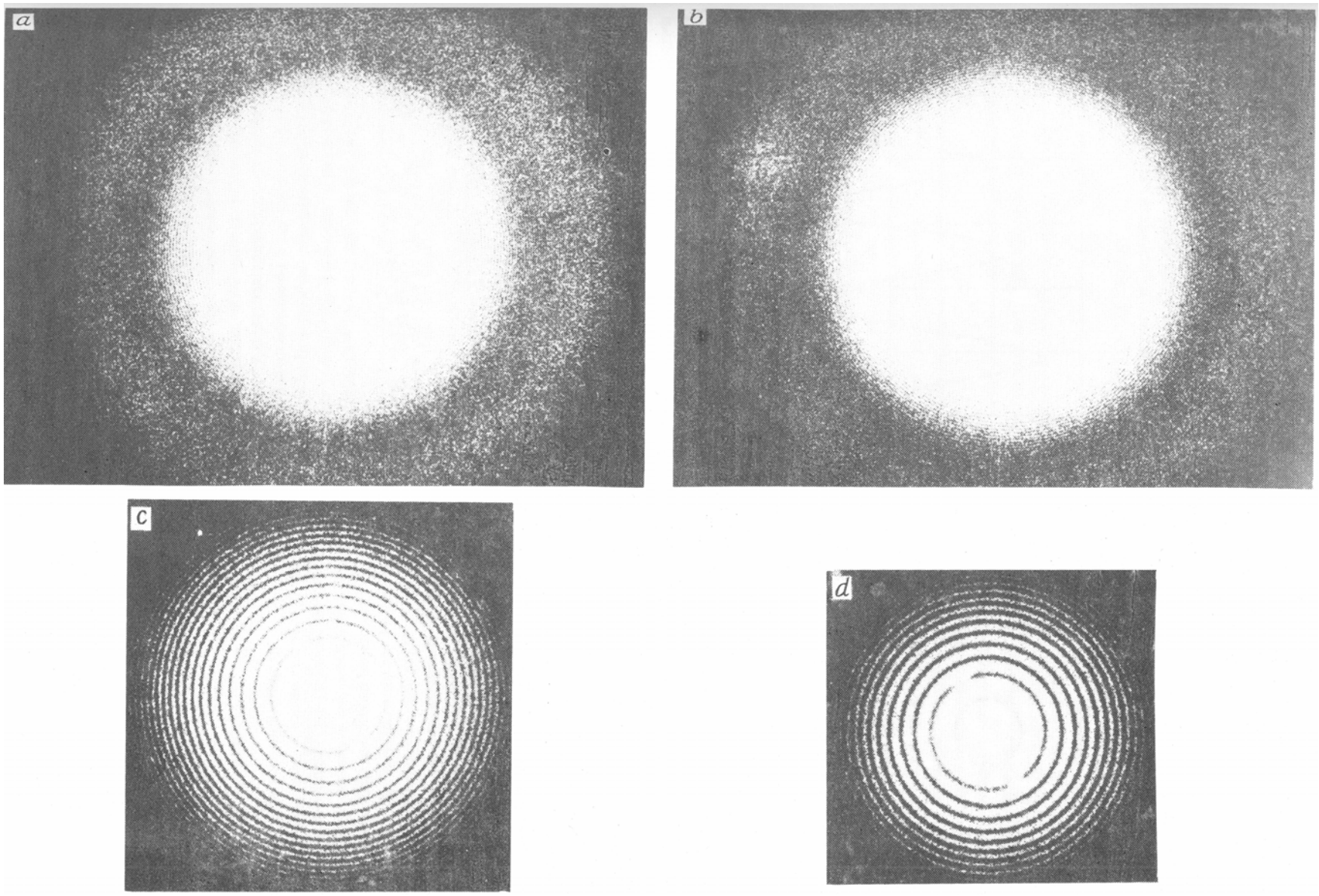

FIG. 3. Photographs of two superimposed patterns in the focal plane of the lens. Exposure increases from (a) to (d)

5. EXPERIMENTAL OBSERVATION OF THE FRESNEL FRINGES

In the experiment we recorded 40 axial holograms of a model medium from different distances. The model medium represented a monolayer of lycopodium particles of radius $R = (15\pm0.5)$ μm. The holograms were recorded by radiation of a He–Ne laser with $\lambda = 0.63$ μm collimated into a parallel beam 30 mm in diameter. The dimensions of the experimental setup provided the fulfillment of the conditions discussed above. That is, the parameter determining the condition of the far field for particles, took the values $0.007 < kR^2/(x_0 - x_j) < 0.03$. A two–dimensional particle number density varied so that the relative area screened by particles was within the limits 0.096 – 0.519. On the one hand, this condition provided low intensity of the scattered field $|\omega| \ll 1$ thereby allowing us to neglect the square term $|\omega|^2$. On the other hand, it provided for statistical independence of particle locations, i.e., an ensemble of particles can be considered as the Poisson one. The regime of exposure and chemical processing of holograms were adjusted to ensure the highest quality of the reconstructed image (Fig. 2).

The processed hologram was illuminated by the same laser beam. Behind the hologram there was a lens 150 mm in diameter, in the focal plane of which ($F = 500$ mm) the intensity distribution was analyzed using a photodiode detector. Two superimposed patterns were observed in the focal plane in complete accordance with conclusions of sections 3 and 4. The "external" pattern completely coincided with a small–angle spectrum of radiation scattered directly by an ensemble of lycopodium particles and was independet of the distances "particles – hologram – lens". The radius of the first dark fringe of the "internal" pattern was related to that of the first Fresnel zone for the particles given by Eq. (27), and the form of the pattern was described by Eq. (26).

The essential difference between the intensities of the central part and fringes of the external pattern (Airy patterns) gives no way to show both superimposed patterns in one photograph. The photographs presented in Fig. 3 were taken with increasing exposure, so that the external pattern is sharply pronounced in Fig. 3*a* while the internal pattern in Fig. 3*d*.

To compare the theoretical and experimental results, it is necessary to make expressions (24)–(26) more specific. For the spherical particles under study it can be easy done by substitution of an explicit form of the scattering amplitude

$$f_R(\rho / F) = 2J_1 (k R \rho / F) / (k R \rho / F), \qquad (28)$$

where J_1 is the Bessel function.

Satisfactory agreement between the theoretical and experimental results is illustrated by Fig. 4. The local disagreements between the calculated and experimental curves can be accounted for by the speckle structure in the focal plane of the lens. This fact was discussed in Ref. 4.

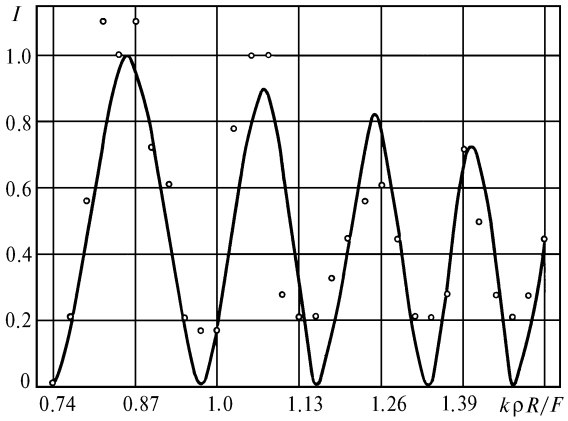

FIG. 4. Comparison of the experimental (points) and calculated (curve) values of the intensity in the focal plane of a lens. Intensity is in relative units, $x_0 - x_j = 35$ cm.

Thus the theoretical and experimental results presented in this paper show that the intensity distribution in the focal plane of the lens contains the information not only about geometrical parameters of the particles, but also about their spatial distribution. This fact can be used for more complete and efficient interpretation of the hologram of the scattering medium.

REFERENCES

1. B.C.R. Ewan, Appl. Opt. **19**, No. 8, 1368–1372 (1980).
2. C.F. Hess and J.D. Trolinger, Opt. Engin. **24**, No. 3, 470–473 (1985).
3. J. Crane, P. Dunn, P.H. Malyak, and B.J. Thomson, SPIE, **348**, 634 (1982).
4. A.G. Borovoy, N.I. Vagin, V.V. Demin, et al., Opt. Atm. **1**, No. 6, 23–28 (1988).
5. S.L. Cartwright, P. Dunn, and B.J. Thomson, Opt. Engin. **19**,
No. 5, 727–733 (1980).